URSI GASS 2020, Rome, Italy, 29 Aug. - 5 Sep. 2020

Experimental Study of Single-Mode Propagation Ranges of Short Waves on Mid-Latitude Radio Paths of Various Lengths

Dmitry V. Ivanov*, Natalya V. Ryabova, Maria I. Ryabova, and Vladimir V. Ovchinnikov
Volga State University of Technology, Yoshkar-Ola, Russian Federation, https://www.volgatech.net

Abstract

Paper presents the findings of experimental research into the single-mode propagation of HF radio waves over long-haul paths by analyzing frequency range where single-mode propagation exists. The influence of various geophysical factors on single-mode propagation range was thoroughly studied. The analysis of the possibilities of the operation of narrowband (3 kHz) and wideband (1 MHz) communication systems in that frequency range is presented.

1 Introduction

Long-haul HF radio communication employing reflection of signals from the ionosphere is highly important in solving the problems of coverage of vast territories of the Earth. However, the ionosphere, being a time and space varying medium, has a number of negative features [1, 2]. They include the interference of signals due to multimode reception and the dependence of the phase velocity of the wave packet spectral components on their frequency (frequency dispersion). To solve these problems, it is reasonable to select the operating frequencies from the single-mode propagation range (SMPR) [4]. Its lower bound is the maximum usable frequency (MUF_2) of the second-order mode and its upper bound is the lowest usable frequency (LUF_P) of the Pedersen ray of the main propagation mode, where the lower ray is at least 20 dB up with respect to the Pedersen ray [4, 5].

It is known [5-7] that the Pedersen ray is unstable mechanism of wave propagation when the wave propagates in the vicinity of the layer maximum. Its propagation is significantly affected by the distribution of the electron concentration. During the periods of ionospheric storms, ionospheric disturbances rise wave attenuation due to the precipitation of radio waves. Maximum usable frequency (MUF) of the higher-order modes follow the MUF of the main mode. Therefore, their variations due to the changes in geophysical conditions are similar. In fact, SMPR characteristics is still poorly studied, because there are multiple effects that influence the wave propagation at frequencies that are SMPR bounds. Nevertheless, HF communication systems employing wideband (up to 1 MHz) signals with frequency-hopping spread spectrum (FHSS) in SMPR can ensure the maximum covertness of the data transmission when the deconvolution method is used to overcome the frequency dispersion. Moreover, employing SMPR for narrowband communications ensures maximum data rate with high noise immunity. Therefore, the studies into the SMPR main characteristics are topical.

2 Wideband channel model, SMPR main parameters and experimental conditions

We assumed that a wideband ionospheric channel with mid-band frequency $\overline{\omega} = (\overline{\omega}_1 + \overline{\omega}_N)/2$ and bandwidth $\Omega_{ch} \sim 0.1 \cdot \overline{\omega}$ consists of the frequency-ordered set of $N = \Omega_{ch} / \omega_{ch} >> 1$ narrowband adjacent partial channels (subchannels) with bandwidth $\omega_{ch} = \omega_k - \omega_{k-1}$ and mid-band frequencies $\overline{\omega}_k = (\omega_k + \omega_{k-1})/2$. Let us denote a random subchannel by the $k \in \{1, N\}$ index that corresponds to the channel mid-band frequency. We also assumed that the frequency dispersion can be neglected in the narrowband partial channel but it should be definitely considered for the wideband channel and the deconvolution method is used to compensate for dispersion at the receiver. Figure 1 illustrates a sketch of a wideband channel.

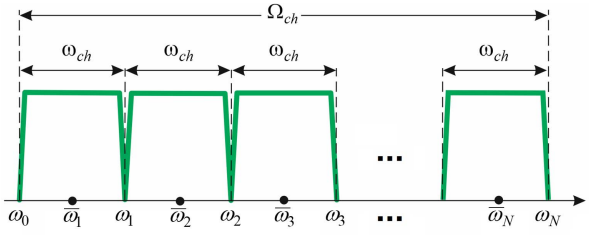

Figure 1. Partial narrowband channels that constitute the wideband channel.

It is clear, that the complex-valued impulse response (IR) of a wideband channel is equal to the sum of IRs of adjacent subchannels:

$$h(\tau) = \frac{1}{2\pi}\left(\int_{\omega_0}^{\omega_1} + \int_{\omega_1}^{\omega_2} + \ldots + \int_{\omega_{k-1}}^{\omega_k} + \ldots + \int_{\omega_{N-1}}^{\omega_N}\right) = \sum_{k=1}^{N} h_k(\tau) = \frac{1}{2\pi}\sum_{k=1}^{N}\int_{\omega_{k-1}}^{\omega_k} H(j\omega)\cdot\exp\, j\omega\tau \cdot d\omega \quad (1)$$

In the framework of this hypothesis, the following equations are used for the frequency response (FR) and phase-frequency response (PFR) of the partial channel:

$$H(\omega) \approx H(\overline{\omega}_k) == const$$
$$\varphi(\omega) \approx \varphi(\overline{\omega}_k) + \varphi'(\overline{\omega}_k) \cdot (\omega - \overline{\omega}_k) \quad (2)$$
$$\varphi'(\overline{\omega}_k) = \tau_{gk}$$

In that case, subchannel IR is as follows:

$$h_k(\overline{\omega}_k, \tau) = \frac{H(\overline{\omega}_k) \cdot \exp(-j\varphi(\overline{\omega}_k))}{2\pi} \cdot \exp(j\omega_k \tau) \cdot$$
$$\cdot \int_{\omega_{k-1}}^{\omega_k} \exp[j(\omega - \overline{\omega}_k)(\tau - \tau_{gk}))] d\omega = \quad (3)$$
$$= \frac{\omega_{ch}}{2\pi} H(j\overline{\omega}_k) \cdot \exp(j\overline{\omega}_k \tau) \cdot \mathrm{sinc}[\omega_{ch}(\tau - \tau_{gk})/2]$$

If the multimode propagation occurs, (3) will contain the sum of such terms. The value $|h_k(\overline{\omega}_k, \tau)|^2$ is the power delay profile (PDP) of a partial channel IR. A frequency-ordered set of PDPs is in function of two variables on the plane of independent variables $(\overline{\omega}_k, \tau)$. It is also referred to as an ionogram. We employed this model for the experimental determination of the ionogram and its interpretation in terms of communication. In fact, in communication, PDP is used to characterize the channel in the fast time. The profile of a sounded subchannel at delays $\tau = \tau_{gk}$ typically has extremums corresponding to the hop propagation modes. Their combination on the ionogram produce tracks of the received modes. With the use of the data on the subchannel PDPs, one can obtain the necessary information on the selected wideband channel. A band of 3...30 MHz that contains an ordered set of narrowband and wideband channels was studied by oblique-incidence sounding (OIS) of the ionospheric communication link.

In the SMPR only single mode is received and, if $SMPR > \Omega_{ch}/2\pi$, there are several adjacent wideband channels. The main SMPR characteristics are: lower bound, upper bound, length and depth of fading (in the frequency domain), slope of the dispersion characteristic. Figures 2(a) and 2(b) show a typical OIS ionogram of a mid-latitude radio path of the length of 2.63 Mm and amplitude-frequency response (AFR) of a HF radio channel with bandwidth of 1 MHz [4]. Red dashed lines indicate SMPR.

Since theoretical approaches to the study of SMPR do not consider all geophysical factors, experimental research methods were used. It was assumed that $\Omega_{ch}/2\pi = 1$ MHz, $\omega_{ch}/2\pi = 10...20$ kHz. There was a particular interest under what geophysical conditions $\Omega_{ch}/2\pi \le SMPR$ is satisfied.

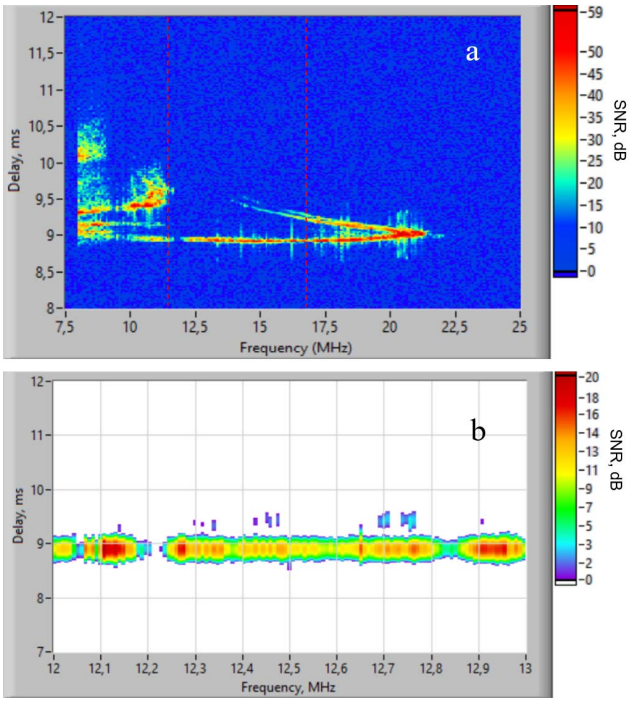

Figure 2. a) OIS ionogram of radio path of length 2.6 Mm recorded at 13/02/19 17:00 (LT) and SMPR; b) AFR of wideband (1 MHz) channel from SMPR.

In the experiments on oblique sounding of the ionosphere by frequency modulated continuous wave (FMCW) signals we used: a receiver located in Yoshkar-Ola and FMCW transmitters located in Cyprus (radio path length D = 2.6 Mm, sounding check point (SCP) located at 43-47° N, main mode 1F2), Inskip (Great Britain) (D = 3.2Mm, SCP 55-57° N, main mode 1F2), Irkutsk (D = 3.6Mm, SCP 57-58° N, main mode 1F2), San Torcas (Spain) (D = 4.1Mm, SCP 44-46° N; 53-55° N, main mode 2F2), Khabarovsk (D = 5.7Mm, SCP 55-56° N; 58-60° N, main mode 2F2).

Reception terminal in Yoshkar-Ola was developed in Volga state university of technology (VSUT) and was based on different technology through the years [8-10]. Over the years of observations, a huge bank of experimental data was gathered. It has been employed in the current research into SMPR.

To study the influence of solar activity on SMPR we selected two periods I, II when the average monthly values of the Wolf numbers were $W_1 \approx 160$, $W_2 \approx 50$. Here, data gathered over the path of the length of 2.6 Mm were used. The influence of the path length, magnetic activity and time of day on SMPR was studied only for the case of the high solar activity $W_1 \approx 160$ with the use of the data gathered from all the radio links.

3 The influence of magnetic activity, time of day, path length on SMPR

Experimental studies into the effect of solar activity on the SMPR were carried out on the path of length of 2.6 Mm. It was found that for the high solar activity ($W_1 = 160$), the average SMPR value was (5.9 ± 0.2) MHz at day and (2.6 ± 0.1) MHz at night. For the low solar activity ($W_2 = 50$), SMPR decreased approximately by 2...3 times and was roughly (2.3 ± 1) MHz at day and (1.3 ± 0.2) MHz at night. However, the SMPR upper bound, divided by the MUF of the radio path, did not change a lot from day to night and was (0.87 ... 0.81) for the high solar activity and (0.74 ... 0.71) for the low one. The lower bound, divided by the MUF of the radio path, did not depend either on the time of day or on the solar activity, and was (0.57 ... 0.68). These data prove that the solar activity changes don't influence SMPR. So, it primarily depends on the MUF of the radio path and the frequency range of the Pedersen ray, i.e. the upper bound of SMPR. The value of SMPR was always observed greater during the day than at night.

Further research was carried out with the use of the data gathered on all the paths during the period of high solar activity ($W_1 = 160$). Figure 3 presents the findings of the research. There is presented the dependence of SMPR on the path length (a - general statistics (mean value ± standard deviation (SD)); b - statistics for the day; c - statistics for the night). The standard deviation for all measurements did not exceed 15%.

Derived from experimental data, analytical models of $SMPR(D)$ for the single-hop paths are $SMPR(D)[MHz] = -2 \cdot D[Mm] + 11.761$ and $SMPR(D) = -D + 5.672$ at day and night respectively. For the two-hop paths they are as follows: $SMPR(D) = -D + 10.724$ and $SMPR(D) = -D + 9.129$.

Estimates showed that for the single-hop radio paths ($D \approx 2.6 \div 3.5$ Mm), SMPR value decreased from 4.25 MHz to 2.65 MHz with the increase in the path length. For the two-hop radio paths ($D \approx 4.0 \div 5.7$ mm), SMPR also decreased from 4.4 MHz to 2.2 MHz with the increase in D. For all the studied radio paths, SMPR value observed at day was greater than at night by roughly 2 ... 2.5 times for the single-hop paths and by 2 ... 5 times for the two-hop paths.

The influence of magnetic activity on SMPR was studied on the basis of a correlation analysis of its variations with the changes in the planetary K-index in the range from 1 to 6 (from quiet to disturbed conditions). It was found no significant correlation between the SMPR value and K-index because $\max CCF \sim 0.32...0.42$ (where CCF is the cross correlation function).

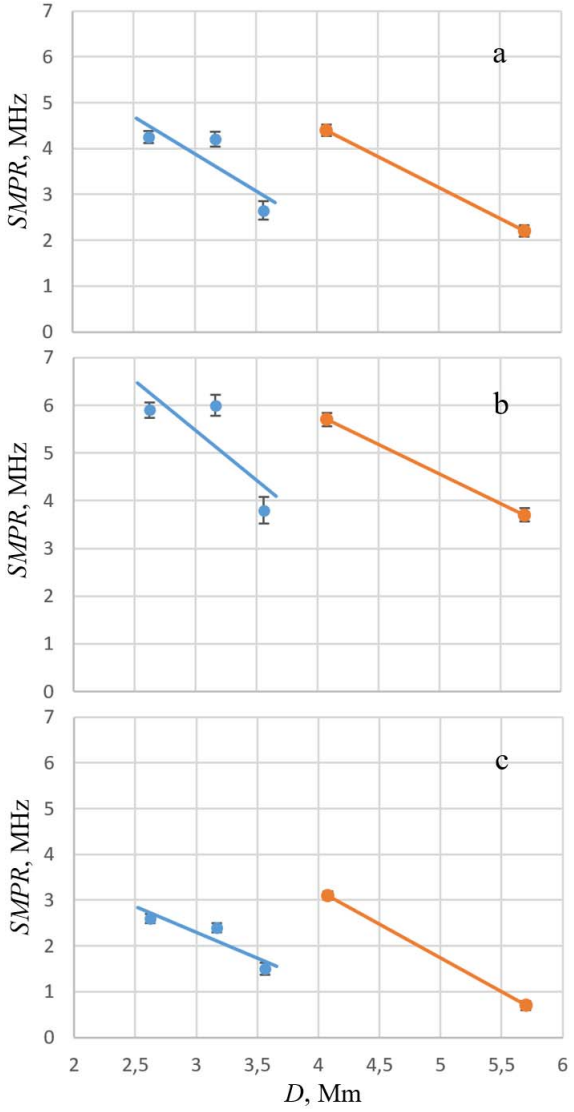

Figure 3. Experimental dependences of SMPR on the path length.

Further research was addressed to narrowband (3 kHz) communication systems and the probability of the presence of a narrowband radio channel with a maximum signal-to-noise ratio (SNR) in the SMPR. Such channel ensures the highest data transfer rate and high noise immunity of the system. Research findings showed that the probability weakly depends on the path length. So, for the path of length of 2.6 Mm, the probability was 0.7; for 3.2 Mm - 0.6; for 3.6 Mm - 0.4; for 4.1 Mm - 0.6; and for 5.7 Mm - 0.5.

For wideband (1 MHz) communication systems, the variations of AFR of wideband channels from SMPR were studied. Obtained data showed that for the studied paths, depth of fading reached up to 15 dB, and fading length was 100 ... 200 kHz. Research findings allowed to conclude that during the high solar activity SMPR can contain up to 6 adjacent channels with 1 MHz bandwidth at day and up to 3 channels at night. But during the low solar activity the number of wideband channels is 2 ... 3 times less.

Therefore, at night, it is not always possible to operate over a 1 MHz bandwidth.

4 Conclusions

The mathematical model of the wideband channel presented in the paper was used for experimental determination of the ionogram and its interpretation in terms of communication. The experiments on OIS over the single-hop paths of length of 2.6 Mm, 3.2 Mm, 3.6 Mm and two-hop paths of length of 4.1 Mm and 5.7 Mm during the periods of different solar activity $W_{1,2} \approx 160$ and 50 were carried out. They allowed to obtain experimental data on the influence of geophysical factors on the single-mode propagation of HF radio waves. It was found that for the high solar activity ($W_1 = 160$), the SMPR average value was (5.9 ± 0.2) MHz at day and (2.6 ± 0.1) MHz at night. During the low solar activity ($W_2 = 50$), SMPR decreased by approximately (2 ... 3) times and was (2.3 ± 1) MHz at day and (1.3 ± 0.2) MHz at night.

The changes in SMPR were mainly influenced by the MUF of the radio path and the frequency range of the Pedersen ray. We derived analytical models of *SMPR*(*D*) dependencies for the period of high solar activity. They showed that for the single-hop radio paths (2.5–3.5 Mm), SMPR value decreased from 4.25 MHz to 2.65 MHz with an increase in the path length. For the two-hop radio paths (4.0–5.5 Mm), SMPR value also decreased from 4.4 MHz to 2.2 MHz with an increase in *D*. For all the studied radio paths, the SMPR value at day was greater than at night by roughly 2 ... 2.5 times for the single-hop paths and by 2 ... 5 times for the two-hop paths. There was no significant correlation between the SMPR and magnetic activity (when K-index changed in the range from 1 to 6).

Research findings showed that for all the paths the narrowband channel with the maximum SNR belonged to SMPR only in half of the cases. For wideband channels with bandwidth of 1 MHz, the variations of AFR did not exceed 15 dB, and the length of fading was 100 ... 200 kHz. Obtained data allowed to conclude that during the high solar activity SMPR can contain up to 6 adjacent channels with 1 MHz bandwidth at day and up to 3 channels at night. But during the low solar activity the number of wideband channels is 2 ... 3 times less. Therefore, at night, it is not always possible to operate over a 1 MHz bandwidth.

5 Acknowledgements

This work was supported by the grant № 18-19-00401 from the Russian Science Foundation.

6 References

1. J. Barona, C. Fernando Quiroga Ruiz, and C. Pinedo, "Implementation of an Electronic Ionosonde to Monitor the Earth's Ionosphere Via a Projected Column through USRP," *Sensors*, 17(5), Apr. 2017, doi:10.3390/s17050946.

2. V. A. Ivanov, N. V. Ryabova, and I. E. Tsarev, "Diagnosing channel scattering function of decameter narrowband stochastic radio channels," *J. Commun. Technol. Electron.*, vol. 55, no. 3, pp. 285-291, 2010 (in Russian).

3. Yu. I. Bova, A. S. Kryukovsky, B. G. Kutuza, and D. S. Lukin, "Investigation of the influence of the earth's ionosphere on the propagation of radio waves in the high frequency range," *Radio Eng. Electron.*, vol. 64, no. 8, pp. 752-758, 2019. (in Russian).

4. V. V. Ovchinnikov, V. A. Ivanov and N. V. Ryabova, "Effect of Season on Single Mode Propagation Band of Short-Wave Signals," *2019 Russian Open Conf. Radio Wave Propag. (RWP)*, Kazan, Russia, 2019, pp. 325-328, doi: 10.1109/RWP.2019.8810376.

5. V. A. Ivanov, N. V. Ryabova, V. P. Uryadov, and V. V. Shumayev, "Propagation of the upper ray in a disturbed ionosphere," *Geomagnetism and Aeronomy*, vol. 35, no. 5, pp. 703-706, Jan. 1996.

6. L. M. Erukhimov, V. P. Uryadov, Yu. N. Cherkashin, V. A. Eremenko, V. A. Ivanov, N. V. Ryabova, and V. V. Shumaev, "Pedersen mode ducting in a randomly stratified ionosphere," *Waves in Random Media*, vol. 7, no. 4, pp. 531-544, Oct. 1997, doi: 10.1080/13616679709409814.

7. A. G. Kim, S. N. Ponomarchuk, G. V. Kotovich, and E. B. Romanova, "Modeling Z-shaped disturbance along the Pedersen ray of oblique sounding ionogram using adaptation of IRI to experimental data," *Sol. Terr. Phys.*, vol. 2, iss. 4, pp. 55-69, 2016, doi: 10.12737/24273.

8. V. A. Ivanov, N. V. Ryabova, V. V. Shumaev, and V. P. Uryadov, "Forecasting and updating HF channel parameters on the basis of oblique chirp sounding," *Radio Sci.*, 32(3), pp. 983-988, 1997, doi: 10.1029/96RS03168.

9. V. A. Ivanov, D. V. Ivanov, N. V. Ryabova, M. I. Ryabova, A. A. Chernov, and V. V. Ovchinnikov, "Studying the parameters of frequency dispersion for radio links of different length using software-defined radio based sounding system," *Radio Sci.*, vol. 54, pp. 34-43, 2019, doi:10.1029/2018RS006636.

10. D. V. Ivanov, V. A. Ivanov, N. V. Ryabova, A. A. Elsukov, R. R. Belgibaev, and V. V. Ovchinnikov, "Universal Ionosonde for Diagnostics of Ionospheric HF Radio Channels and Its Application in Estimation of Channel Availability," *Proc. 12th Eur. Conf. Antennas Propag. (EuCAP 2018)*, vol. 2018, iss. CP741, pp. 1-5, doi: 10.1049/cp.2018.0473.